Electronic Supplementary Information

Potassium-ion-responsive chiral supramolecular hydrogels exhibiting long-range chirality transfer from D- or L-alanine to achiral frameworks

Atsuna Kondo,[a] Hisako Sato,[b] Akitaka Ito,[c,d] Yoshiro Kondo,[e] Shingo Hadano,[a,f,g] Kiyonori Takahashi,[h] Sun Dekura,[i] Jun Manabe,[j] Tetsu Sato,[i] Tomoyuki Akutagawa,[i] Takayoshi Nakamura,[j,k] Sadafumi Nishihara,[j] Masayuki Izumi [a,e,f] and Rika Ochi *[a,e,f]

[a.] *Graduate School of Integrated Arts and Sciences, Kochi University, 2-5-1, Akebono-cho, Kochi 780-8520, Japan. E-mail: ochi@kochi-u.ac.jp*

[b.] *Faculty of Science, Ehime University, 2-5, Bunkyo-cho, Matsuyama 790-8577 Japan.*

[c.] *School of Engineering Science, Kochi University of Technology, Kami, Ko-chi 782-8502, Japan.*

[d.] *Research Center for Advanced Chital Optical Materials (RACOMs), Kochi University of Technology, Kami, Kochi 782-8502, Japan.*

[e.] *JASCO Corporation, 2967-5, Ishikawa-machi, Hachioji, Tokyo 192-8537, Japan.*

[f.] *Faculty of Science and Technology, Kochi University, 2-5-1, Akebono-cho, Kochi 780-8520, Japan.*

[g.] *Research and Education Faculty, Kochi University, 2-5-1, Akebono-cho, Kochi 780-8520, Japan.*

[h.] *Faculty of Advanced Science and Technology, Kumamoto University, 2-39-1, Kurokami, Chuo-ku, Kumamoto 860-8555, Japan.*

[i.] *Institute of Multidisciplinary Research for Advanced Materials (IMRAM), Tohoku University, 2-1-1, Katahira, Aoba-ku, Sendai 980-8577, Japan.*

[j.] *Department of Chemistry, Graduate School of Advanced Science and Engineering, Hiroshima University, 1-3-1, Kagamiyama, Higashi-hiroshima 739-8526, Japan.*

[k.] *Research Institute for Electronic Science (RIES), Hokkaido University, N20W10, Kita-ku, Sapporo 001-0020, Japan.*

Materials and Methods

Generals

Chemical reagents were purchased from Tokyo Chemical Industry Co., Ltd., FUJIFILM Wako Pure Chemical Co., or Watanabe Chemical Industries, Ltd., and used without further purification. Thin layer chromatography (TLC) was performed on TLC silica gel $60F_{254}$ (Merck). Column chromatography was performed on silica gel 60N (Kanto Chemical Co., Inc., spherical neutral, 63–210 μm). ^{1}H NMR and ^{13}C NMR spectra in CD_3OD were recorded on a JEOL ECA500 spectrometer, and chemical shifts were determined by residual non-deuterated solvent as the internal reference. Peak multiplicities are abbreviated as follows: s = singlet, d = doublet, t = triplet, q = quartet, m = multiplet, dd = double doublet, and br = broad. LRMS (ESI-MS) analyses were carried out using a Bruker amaZon SL mass spectrometer. FT-IR spectra (for chemical structure identification of compounds) were recorded on a JEOL FT/IR-4100 spectrometer using KBr pellets in the range of 4000 to 500 cm^{-1}, with a resolution of 4 cm^{-1}.

Preparation of solutions of compounds

Gelators (typically 1.0 mg) were suspended in 0.2 M Tris–HCl buffer (pH 8.0) in screw-capped glass vials (Maruemu Corp., cat. no. 0102-02). The suspension was heated until complete dissolution, then cooled to room temperature (approximately 25 °C) and incubated for approximately 10 min.

Preparation of hydrogels

Hydrogels were prepared by adding 1.0 equiv. KCl to the gelator solutions in 0.2 M Tris–HCl buffer (pH 8.0) at concentrations appropriate for each measurement. The mixtures were gently mixed and then incubated at room temperature (approximately 25 °C) for 5 min to allow complete gelation.

VCD and IR measurements of gelator solutions and hydrogels

VCD and IR absorption spectra were recorded on a custom-built spectrometer (MultiD-MIRAI-2020) developed in collaboration with JASCO Corporation, Japan. Measurements were performed in FT-VCD mode with standard cell alignment. Samples of **B15C5-AAC-C6-L-Ala** and **B15C5-AAC-C6-D-Ala** (60 mM) were prepared in 0.2 M Tris–DCl buffer (pD 8.0). Hydrogels of the L- (L-gel) and D-enantiomer (D-gel) were obtained by addition of 1.0 equiv. KCl, whereas the L-enantiomer solution (L-sol) was measured without KCl addition. An aliquot (5 μL) of each sample was placed between two CaF_2 windows separated by a 50 μm Teflon spacer. Spectra were acquired by accumulating 10,000 scans at 25 °C. Baseline correction was performed using a reference spectrum recorded under identical conditions with the same CaF_2 windows. Corrected VCD spectra were subsequently normalised to optical density.

CD and UV–Vis measurements of gelator solutions and hydrogels

CD and UV–Vis spectra were recorded on a JASCO J-1500 CD spectrometer with a data interval of 0.1 nm. An aliquot (20 μL) of each sample was placed in an assembled quartz cell with a path length of 0.1 mm (GL Sciences Inc., cat. no. AB10-UV-0.1) using a dedicated cell adaptor (GL Sciences Inc., cat. no. CAS-10-1). Baseline correction was performed by subtracting the spectrum of the buffer.

DFT calculations

Theoretical calculations were performed using Gaussian 16W (Revision A.03) software.[1] Ground-state geometries of monomer and tetramer of *N*-Ac-L-Ala were optimised under the B3LYP/6-31G(d,p) level, incorporating Grimme's D3 empirical dispersion correction to account for weak intermolecular interactions,[2] as in water by using a conductor-like polarizable continuum model (CPCM).[3] Carboxylate forms were assumed for mono- and tetrameric *N*-Ac-L-Ala on the basis of the crystal structures of L- and D-Ala. Frequency

calculations for the optimized geometries by identical methodologies were then performed. It is noted that no negative frequency was obtained, irrespective of the ion. For comparison, the frequency calculation for the L- or D-Ala tetramer was performed for a tetramer in the reported crystal structure obtained from the CCDC database,[4] without structural optimisation and as in vacuum. Simulated IR and VCD spectra were obtained from calculated vibrational rotational strengths and converted to Lorentzian bands (HWHM = 4 cm^{-1}) by using GaussView 6.0.[5] Ground-state geometry of a carboxylate form of **B15C5-AAC-C6-L-Ala** was also optimised under the B3LYP/6-31G(d,p) level, as in water by using CPCM.

TEM analysis of xerogels

Hydrogel samples (40 mM in 0.2 M Tris–HCl buffer (pH 8.0) containing 1.0 equiv. KCl) were drop-cast (5 μL) onto a carbon-coated copper TEM grid (EM Japan Co., LTD., cat. no. U1013) placed on filter paper. Excess solution was immediately removed using the underlying filter paper. The grid was then washed with water (5 μL × 2) and dried under reduced pressure for 6 h. TEM images were acquired using a Hitachi H-7100 microscope at an accelerating voltage of 100 kV and equipped with a CCD camera and AMTV600 software.

SEM analysis of xerogels

Hydrogel samples (40 mM in 0.2 M Tris–HCl buffer (pH 8.0) containing 1.0 equiv. KCl) were drop-cast (5 μL) onto glass substrates prepared by cutting microscope slides (Matsunami Glass Ind., Ltd., cat. no. S1126) into approximately 1 cm^2 pieces. Excess solution was removed using filter paper, followed by washing with water (5 μL × 2) and drying under reduced pressure for 6 h. Dried samples were coated with a 3 nm gold layer by vapor deposition prior to imaging. SEM images were acquired using a JEOL JSM-6510 microscope operated at an accelerating voltage of 1.0 kV.

PXRD analysis of B15C5-AAC-C6-L-Ala hydrogel (L-gel)

A hydrogel sample of **B15C5-AAC-C6-L-Ala** (60 mM in 0.2 M Tris–HCl buffer (pH 8.0) containing 1.0 equiv. KCl) was placed onto a non-reflective sample holder consisting of a single-crystal Si plate with a diameter of 5 mm and a depth of 0.1 mm. PXRD patterns were recorded on a Rigaku SmartLab SE X-ray diffractometer with Cu Kα radiation (λ = 1.5418 Å), operated at 40 kV and 50 mA with a 2 mm slit. Data were collected over a 2θ range of 2 to 15° at a scan rate of 0.1° min^{-1} with a step size of 0.01°. PXRD patterns of Tris–HCl and KCl were also recorded under identical measurement conditions to confirm that the observed diffraction peaks originated from the hydrogel structure. The PXRD patterns shown in the figures are background-subtracted.

Synthesis

Cl-AAC-C6-COOH was synthesized following a previously reported procedure.[6] The purification method for **B15C5-AAC-C6-COOH** was improved from the earlier previous report[7] and is described herein. Full spectroscopic characterisation data (^{1}H NMR, ^{13}C NMR, LRMS, and IR spectra) for final compounds are provided in Figs. S9–S16.

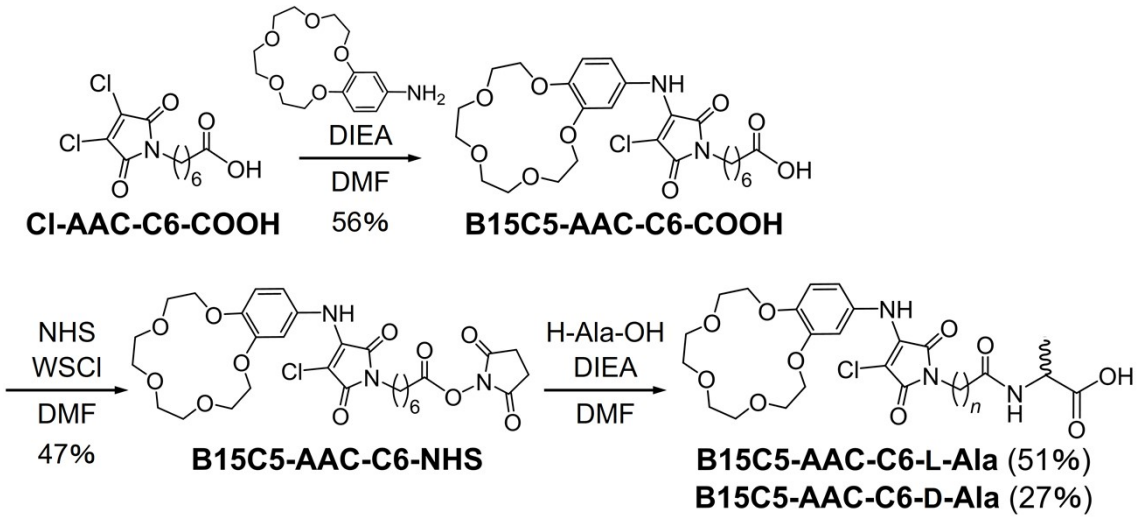

Scheme S1. Synthesis of **B15C5-AAC-C6-L-Ala** and **B15C5-AAC-C6-D-Ala**.

Synthesis of B15C5-AAC-C6-COOH[7]: To a solution of **Cl-AAC-C6-COOH**[6] (150 mg, 0.51 mmol) in dry *N*, *N*-dimethylformamide (DMF, 2 mL) were added 4'-aminobenzo-15-crown-5-ether (159 mg, 0.56 mmol, 1.1 equiv.) and *N*,*N*-diisopropylethylamine (DIEA, 110 μL, 0.64 mmol, 1.25 equiv.). The reaction mixture was stirred overnight at room temperature under a nitrogen atmosphere. The crude mixture was diluted with ethyl acetate (EtOAc, 60 mL) and washed with 1M hydrochloric acid (15 mL × 4). The organic phase was collected, dried over anhydrous $MgSO_4$, and filtered. The filtrate was concentrated under reduced pressure, and the resulting residue was purified by reprecipitation from diethyl ether. The solid was further dried under reduced pressure to afford **B15C5-AAC-C6-COOH** (153 mg, 56%) as a yellow powder. ^{1}H NMR (500 MHz, CD_3OD): δ (ppm) = 1.29–1.42 (m, 4H), 1.58–1.64 (m, 4H), 2.27 (t, J = 7.5 Hz, 2H), 3.52 (t, J = 6.9 Hz, 2H), 3.71–3.74 (m, 8H), 3.87–3.88 (m, 4H), 4.12–4.15 (m, 4H), 6.77 (dd, J_1 = 2.3 Hz, J_2 = 8.6 Hz, 1H), 6.85 (d, J = 2.3 Hz, 1H), and 6.95 (d, J = 8.6 Hz, 1H). HRMS (ESI, positive mode): Calcd. for $[M(C_{25}H_{33}ClN_2O_9) + Na]^+$: m/z = 563.1762; Found: 563.1767. FT-IR (KBr pellet): ν = 3263.9, 3235.0, 2937.1, 2852.2, 1766.5, 1721.2, 1660.0, 1603.5, 1514.8, 1440.6, 1415.5, 1373.1, 1331.6, 1295.9, 1237.1, 1193.7, 1137.8, 1080.9, 1000.9, 981.6, 965.2, 939.2, 907.3, 874.6, 850.5, 937.4, 907.3, 874.6, 850.5, 797.4, 741.5, 650.9, 629.6, 525.5 cm^{-1}.

Synthesis of B15C5-AAC-C6-NHS: To a solution of **B15C5-AAC-C6-COOH** (153 mg, 0.28 mmol) in dry DMF (2 mL) were added *N*-hydroxysuccinimide (NHS, 49 mg, 0.43 mmol, 1.5 eq.) and 1-(3-dimethylaminopropyl)-3-ethylcarbodiimide hydrochloride (WSCI ・ HCl, 107 mg, 0.56 mmol, 2.0 eq.). The reaction mixture was stirred overnight at room temperature under a nitrogen atmosphere. The crude mixture was diluted with dichloromethane (CH_2Cl_2, 60 mL) and washed with water (15 mL × 3). The organic phase was collected, dried over anhydrous $MgSO_4$, and filtered. The filtrate was concentrated, and the crude product was purified by column chromatography (SiO_2, CH_2Cl_2:MeOH = 20:1 to 6:1 (v/v)). The purified fraction was concentrated and dried under reduced

pressure to afford **B15C5-AAC-C6-NHS** (84.2 mg, 47%) as an orange viscous liquid. ^{1}H NMR (500 MHz, CD_3OD): δ = 1.29–1.49 (m, 4H) 1.57–1.64 (m, 2H), 1.69–1.75 (m, 2H), 2.62 (t, J = 7.2 Hz, 2H), 2.82 (s, 4H), 3.51 (t, J = 7.0 Hz, 2H), 3.68–3.74 (m, 8H), 3.86–3.87 (m, 4H), 4.10–4.12 (m, 4H), 6.75 (dd, J_1 = 2.6 Hz, J_2 = 6.7 Hz, 1H), 6.82 (d, J = 2.3 Hz, 1H), 6.92 (d, J = 8.6 Hz, 1H). ^{13}C NMR (125 MHz, CD_3OD): δ (ppm) = 25.56, 26.28, 26.49, 27.26, 29.20, 29.41, 31.46, 39.07, 61.91, 70.37, 70.44, 70.58, 71.29, 71.37, 71.85, 91.99, 112.13, 114.76, 118.24, 131.59, 139.66, 148.48, 150.02, 167.05, 169.76, 170.22, 171.84, 174.86. LRMS (ESI, positive mode): Calcd. for $[M(C_{29}H_{36}ClN_3O_{11}) + Na]^+$: *m/z* = 660.2; Found: 660.2. FT-IR (KBr pellet): ν = 3296.7, 2938.0, 2866.7, 1812.8, 1781.9, 1737.6, 1714.4, 1654.6, 1601.6, 1557.2, 1515.8, 1439.6, 1410.7, 1362.5, 1294.0, 1265.1, 1237.1, 1205.3, 1133.9, 1106.9, 1066.4, 983.5, 936.3, 876.5, 851.4, 811.9, 784.9, 743.4, 649.9, 570.8, 526.5 cm^{-1}.

Synthesis of B15C5-AAC-C6-L-Ala: To a solution of **B15C5-AAC-C6-NHS** (42.1 mg, 0.07 mmol) in DMF (2 mL) were added L-alanine (7.7 mg, 0.09 mmol, 1.3 eq.) and DIEA (14.2 μL, 0.08 mmol, 1.25 eq.). The reaction mixture was stirred at 40 °C overnight under a nitrogen atmosphere. The crude mixture was diluted with CH_2Cl_2 (60 mL) and washed with 5% aqueous citric acid (20 mL × 5). The organic phase was collected, dried over anhydrous $MgSO_4$, and filtered. The filtrate was concentrated, and the crude product was purified by column chromatography (SiO_2, CH_2Cl_2:MeOH = 12:1 to 3:1 to 0:1 (*v*/*v*)). The purified fraction was concentrated under reduced pressure, and the resulting residue was purified by reprecipitation from diethyl ether. The solid was further dried under reduced pressure to afford **B15C5-AAC-C6-L-Ala** (21.9 mg, 51%) as an orange powder. ^{1}H NMR (500 MHz, CD_3OD): δ (ppm) = 1.29–1.41 (m, 7H), 1.57–1.65 (m, 4H), 2.23 (t, J = 7.5 Hz, 2H), 3.52 (t, J = 7.0 Hz, 2H), 3.71–3.75 (m, 8H), 3.87–3.89 (m, 4H), 4.16–4.19 (m, 4H), 4.22 (q, J = 7.3 Hz, 1H), 6.80 (dd, J_1 = 2.3 Hz, J_2 = 6.8 Hz, 1H), 6.88 (d, J = 2.4 Hz, 1H), 7.00 (d, J = 8.5 Hz, 1H). ^{13}C NMR (125 MHz, CD_3OD): δ (ppm) = 18.76, 26.77, 27.53, 29.53, 29.77, 36.96, 39.13, 51.29, 69.65, 70.07, 70.11, 70.21, 70.80, 70.86, 71.23,

71.27, 92.20, 112.23, 114.92, 118.53, 131.93, 139.65, 148.07, 149.67, 167.00, 169.70, 175.40, 179.97. LRMS (ESI, positive mode): Calcd. for $[M(C_{28}H_{38}ClN_3O_{10}) + Na]^+$: *m/z* = 634.2; Found: 634.2. FT-IR (KBr pellet): *v* = 3422.1, 2932.2, 2864.7, 1771.3, 1715.4, 1653.7, 1604.5, 1558.2, 1509.0, 1456.0, 1409.7, 1361.5, 1292.1, 1262.2, 1243.9, 1230.4, 1192.8, 1131.1, 1106.0, 1079.0, 1048.1, 931.5, 866.8, 850.5, 833.1, 771.4, 750.2 cm^{-1}.

Synthesis of B15C5-AAC-C6-D-Ala: To a solution of **B15C5-AAC-C6-NHS** (42.1 mg, 0.07 mmol) in DMF (2 mL) were added D-alanine (7.8 mg, 0.09 mmol, 1.3 eq.) and DIEA (14.2 μL, 0.08 mmol, 1.25 eq.). The reaction mixture was stirred at 40 °C overnight under a nitrogen atmosphere. The crude mixture was diluted with CH_2Cl_2 (60 mL) and washed with 5% aqueous citric acid (20 mL × 5). The organic phase was collected, dried over anhydrous $MgSO_4$, and filtered. The filtrate was concentrated, and the crude product was purified by column chromatography (SiO_2, CH_2Cl_2:MeOH = 12:1 to 3:1 to 0:1). The purified fraction was concentrated under reduced pressure, and the resulting residue was purified by reprecipitation from diethyl ether. The solid was further dried under reduced pressure to afford **B15C5-AAC-C6-D-Ala** (11.7 mg, 27%) as an orange powder. ^1H NMR (500 MHz, CD_3OD): δ (ppm) = 1.29–1.39 (m, 7H), 1.58–1.65 (m, 4H), 2.23 (t, *J* = 7.6 Hz, 2H), 3.52 (t, *J* = 7.0 Hz, 2H), 3.71–3.75 (m, 8H), 3.87–3.89 (m, 4H), 4.15–4.17 (m, 4H), 4.22 (q, *J* = 7.3 Hz, 1H), 6.79 (dd, J_1 = 2.5 Hz, J_2 = 6.8 Hz, 1H), 6.87 (d, *J* = 2.3 Hz, 1H), 6.98 (d, *J* = 8.7 Hz, 1H). ^{13}C NMR (125 MHz, CD_3OD): δ (ppm) = 18.69, 26.78, 27.54, 29.54, 29.77, 36.94, 39.14, 51.26, 69.69, 70.12, 70.15, 70.25, 70.86, 70.92, 71.31, 71.34, 92.17, 112.23, 114.90, 118.51, 131.90, 139.67, 148.13, 149.71, 167.01, 169.70, 175.44, 180.01. LRMS (ESI, positive mode): Calcd. for $[M(C_{28}H_{38}ClN_3O_{10}) + Na]^+$: *m/z* = 634.2; Found: 634.2. FT-IR (KBr pellet): *v* = 3416.3, 2934.2, 2863.8, 1771.3, 1716.3, 1653.7, 1604.5, 1558.2, 1509.0, 1457.0, 1409.7, 1361.5, 1292.1, 1260.3, 1242.9, 1228.4, 1194.7, 1130.1, 1096.3, 1076.1, 1046.2, 933.4, 882.6, 852.4, 831.2, 771.4, 749.2 cm^{-1}.

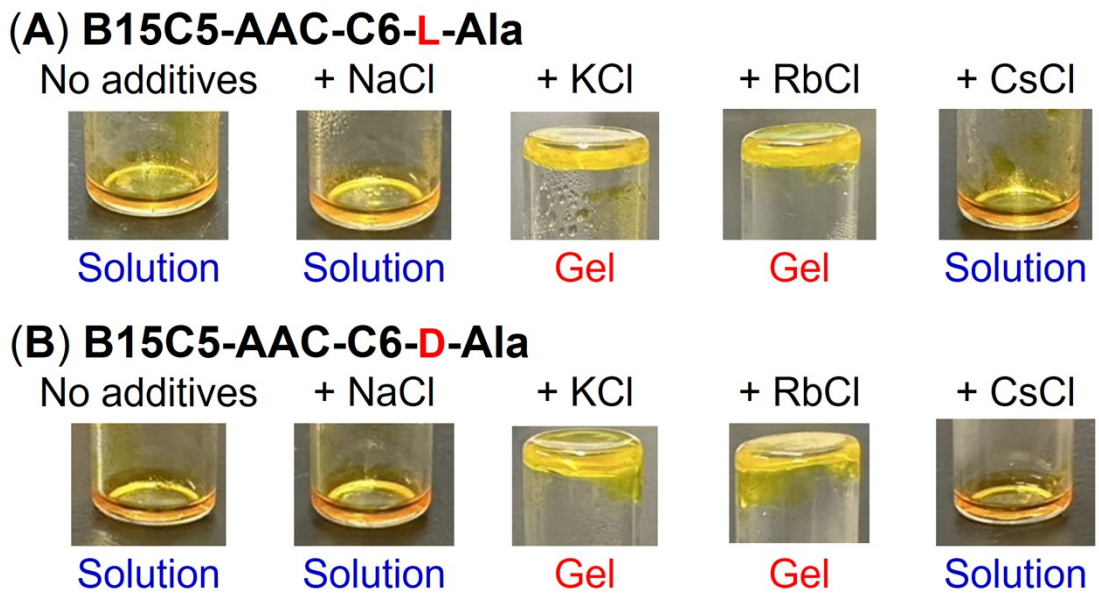

Fig. S1. Photographs of (A) **B15C5-AAC-C6-L-Ala** and (B) **B15C5-AAC-C6-D-Ala** after the addition of alkali metal chlorides (NaCl, KCl, RbCl, and CsCl). Conditions: [gelator] = 60 mM, [alkali metal chloride] = 0 or 66 mM (1.1 equiv.) in 0.2 M Tris–HCl buffer (pH 8.0).

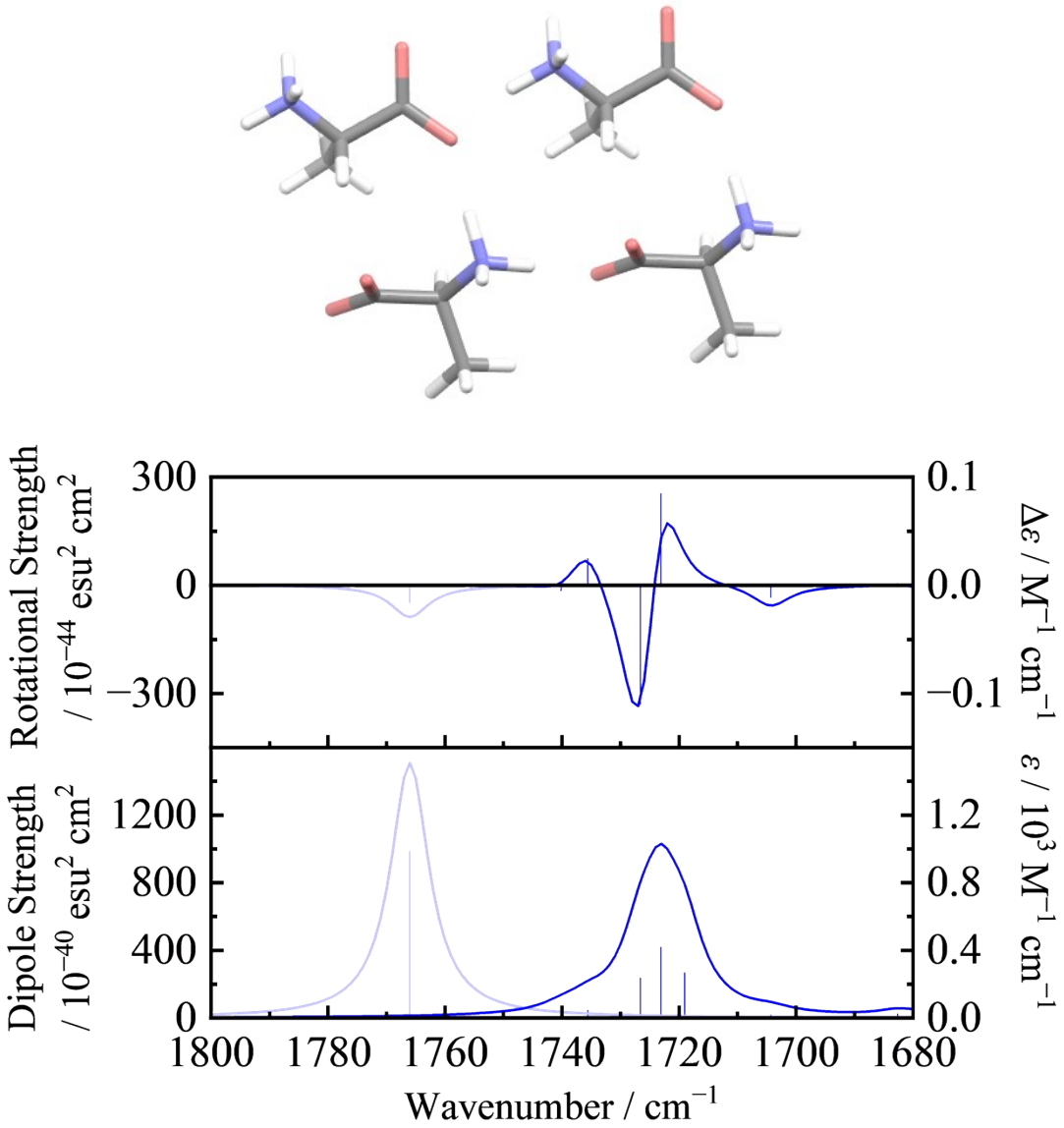

Figure S12. Structure of the L-Ala tetramer in the crystalline phase (top, CCDC number: 278467)[4] and calculated VCD and IR spectra (bottom) of the L-tetramer (blue) and the optimised zwitterionic L-alanine (pale blue). The VCD and IR intensities of the tetramer are divided by four to enable direct comparison with those of the monomer.

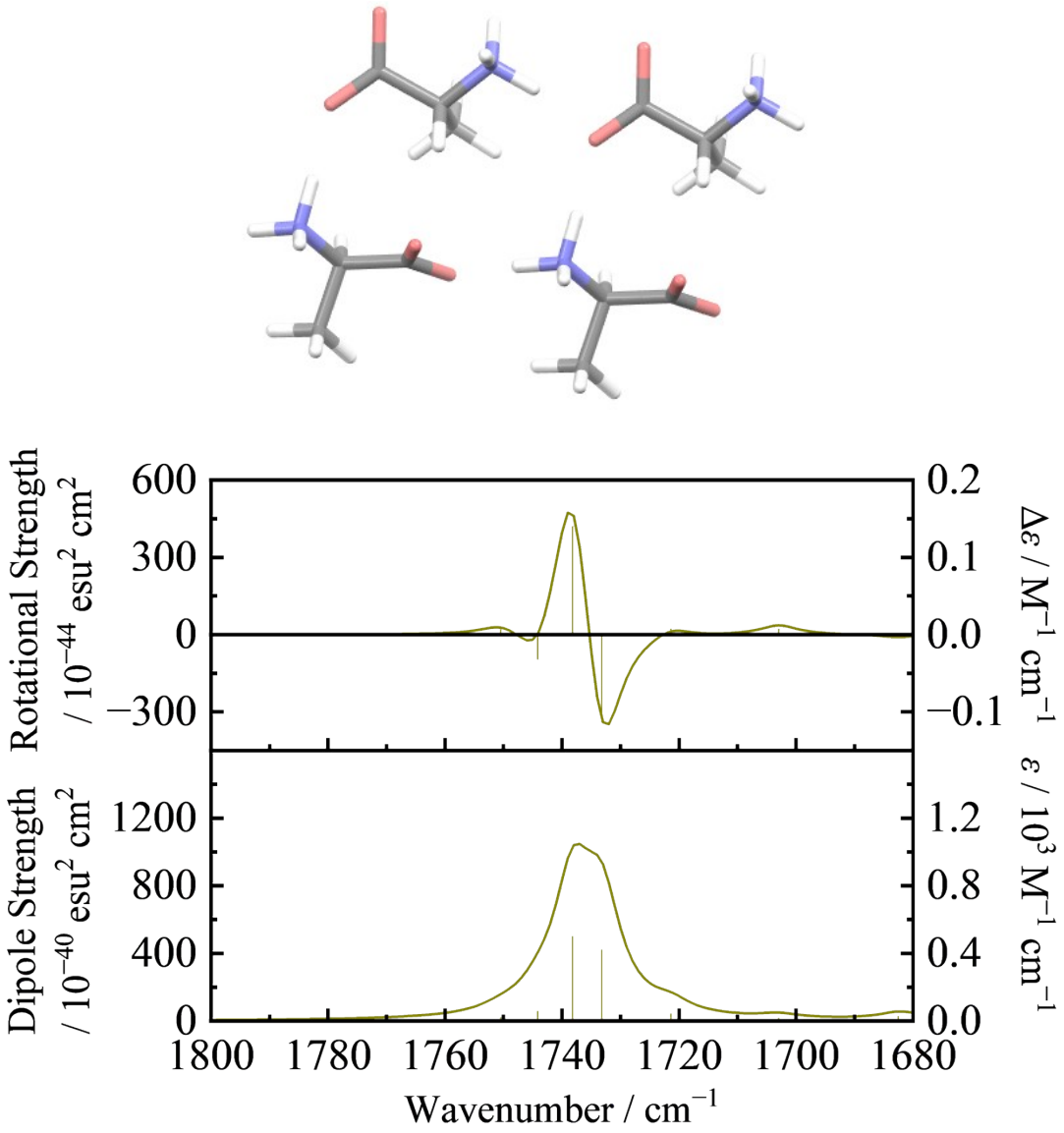

Figure S23. Structure of the D-Ala tetramer in the crystalline phase (top, CCDC number: 278466)[4] and calculated VCD and IR spectra (bottom) of the D-tetramer. The VCD and IR intensities of the tetramer are divided by four to enable direct comparison with those of the monomer.

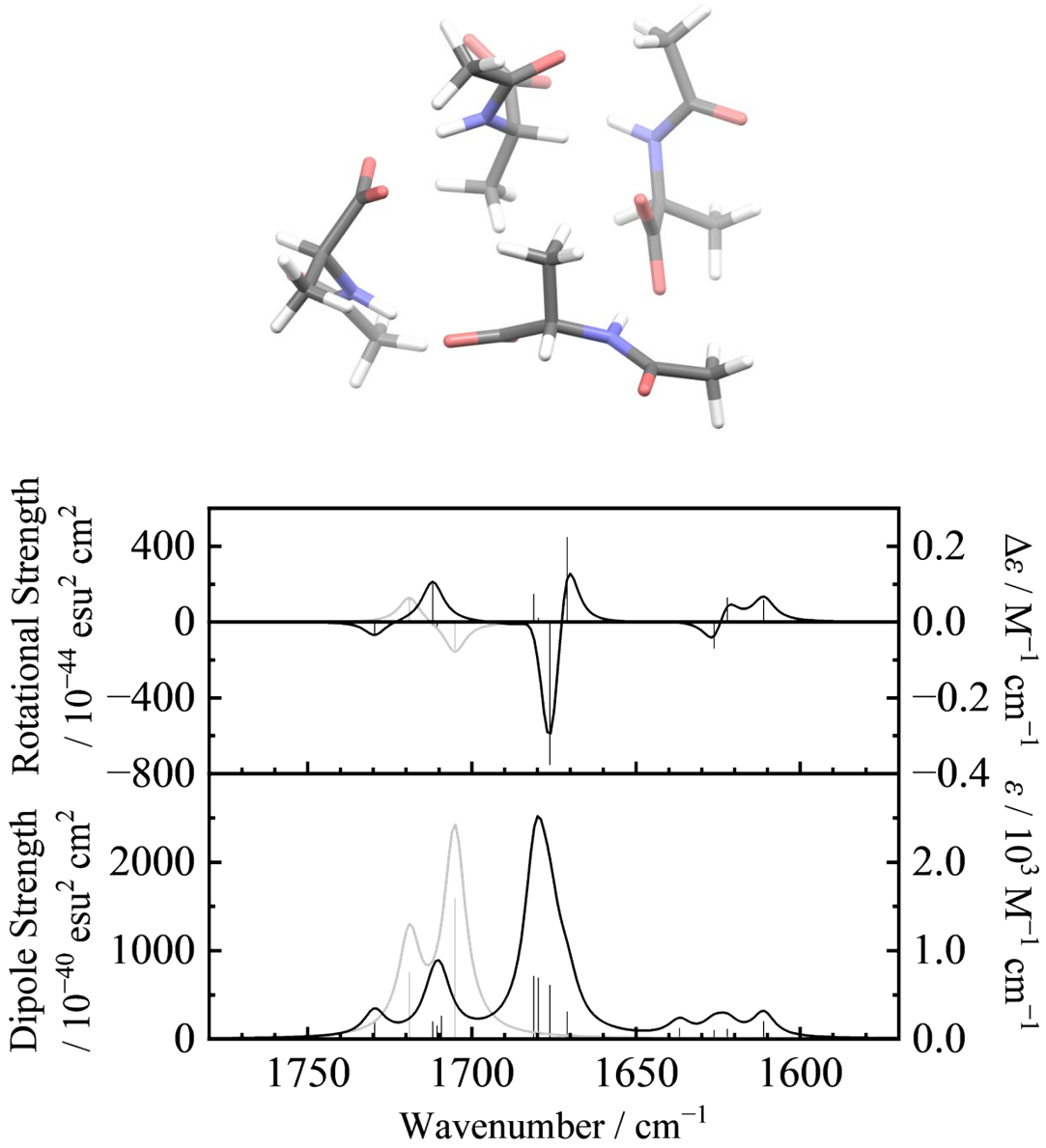

Figure S34. Structure of the optimised *N*-Ac-L-Ala (carboxylate form) tetramer (top) and calculated VCD and IR spectra (bottom) of *N*-Ac-L-Ala tetramer (black) and monomer (grey). The VCD and IR intensities of the tetramer are divided by four to enable direct comparison with those of the monomer.

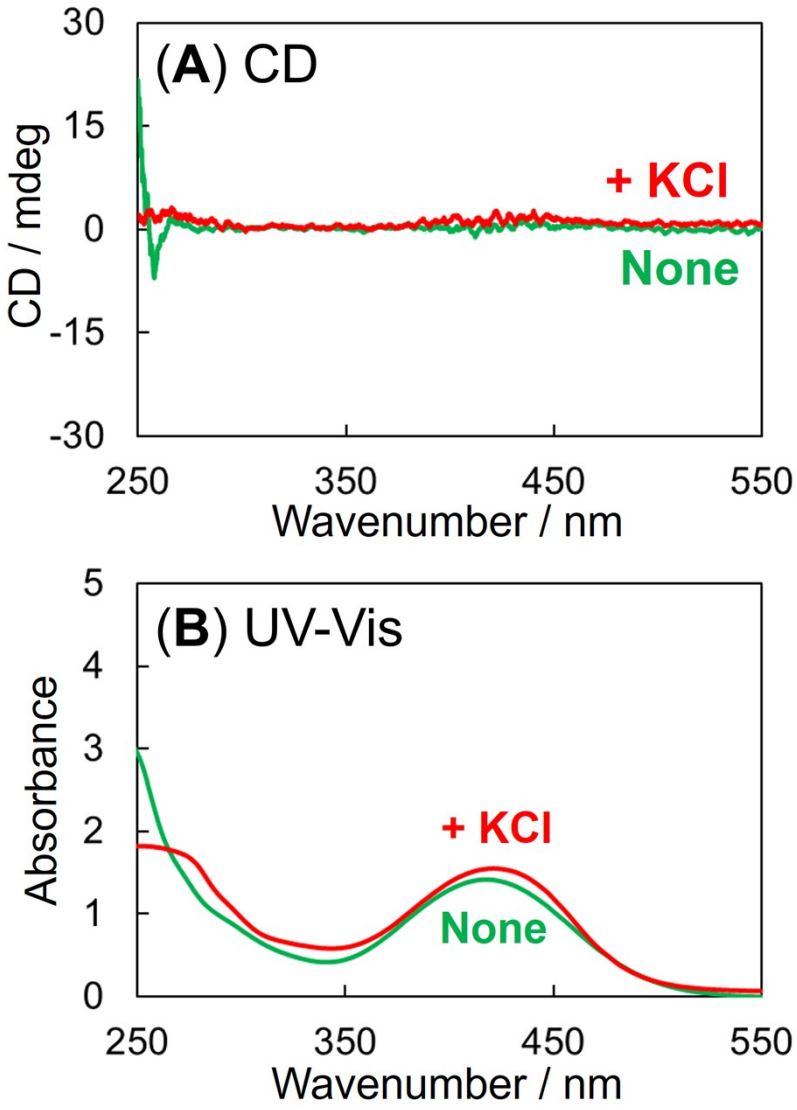

Figure S45. (A) CD and (B) UV-Vis spectra of achiral gelator **B15C5-AAC-C6-COOH** in the absence (green) and presence (red) of 1.0 equivalent of KCl. Conditions: [**B15C5-AAC-C6-COOH**] = 25 mM, [KCl] = 0 or 25 mM in 0.2 M Tris-HCl buffer (pH 8.0).

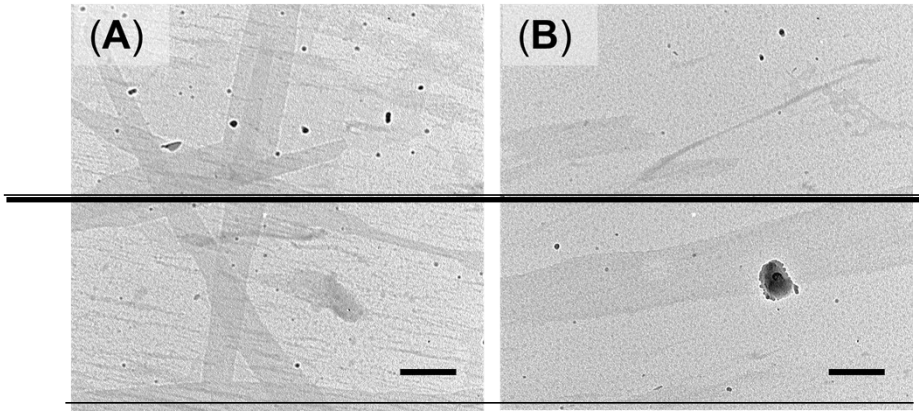

~~**Figure S5.** Representative TEM images of (A) **B15C5-AAC-C6-L-Ala** and **B15C5-AAC-C6-D-Ala** hydrogels, deposited on carbon-coated grids. Scale bar: 500 nm. Conditions: [**B15C5-AAC-C6-L/D-Ala**] = [KCl] = 40 mM in 0.2 M Tris–HCl buffer (pH 8.0).~~

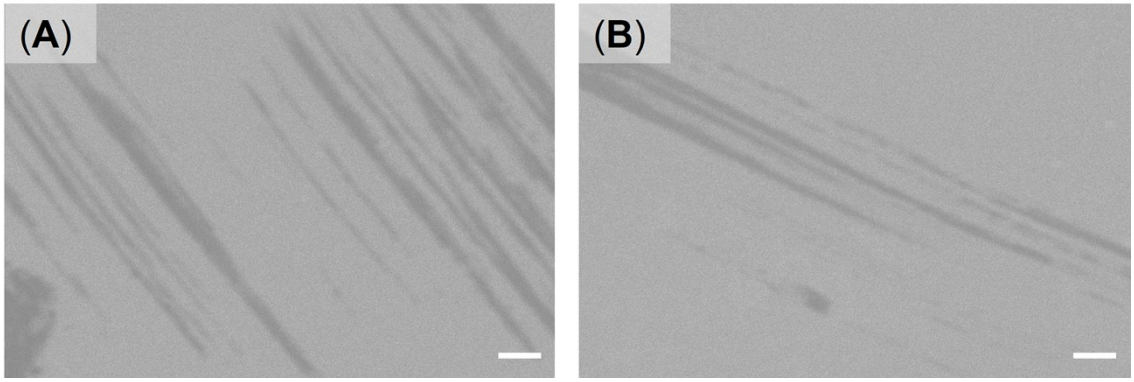

Figure S6. Representative SEM images of (A) **B15C5-AAC-C6-L-Ala** and **B15C5-AAC-C6-D-Ala** hydrogels, deposited on glass substrates. The samples were coated with a 3 nm gold layer by sputter deposition. Scale bar: 500 nm. Conditions: [**B15C5-AAC-C6-L/D-Ala**] = [KCl] = 40 mM in 0.2 M Tris–HCl buffer (pH 8.0).

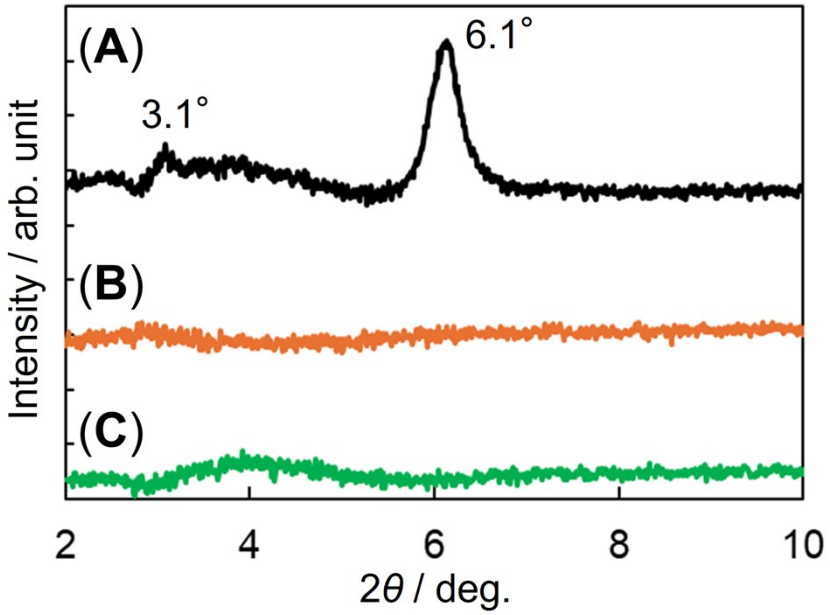

Figure S7. PXRD analysis of **B15C5-AAC-C6-L-Ala** hydrogel (A), KCl (B) and Tris–HCl (C). Conditions: [**B15C5-AAC-C6-L-Ala**] = [KCl] = 60 mM in 0.2 M Tris–HCl buffer (pH 8.0).

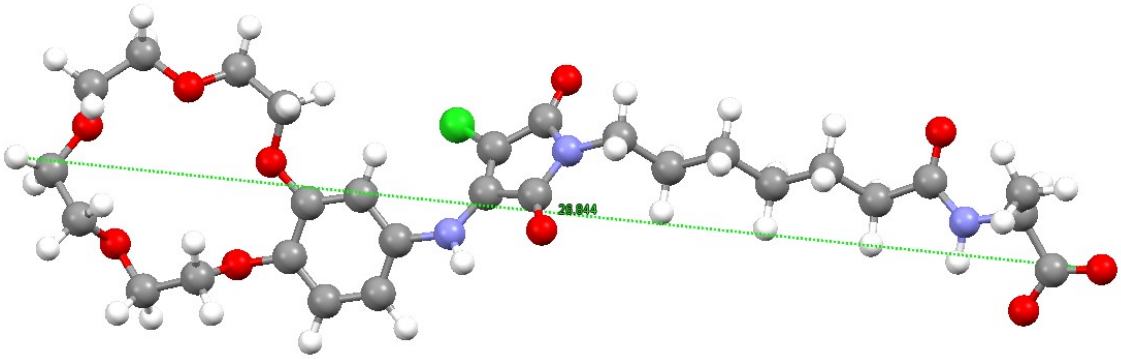

Figure S8. DFT-optimised structure of the deprotonated **B15C5-AAC-C6-L-Ala** (monomer).

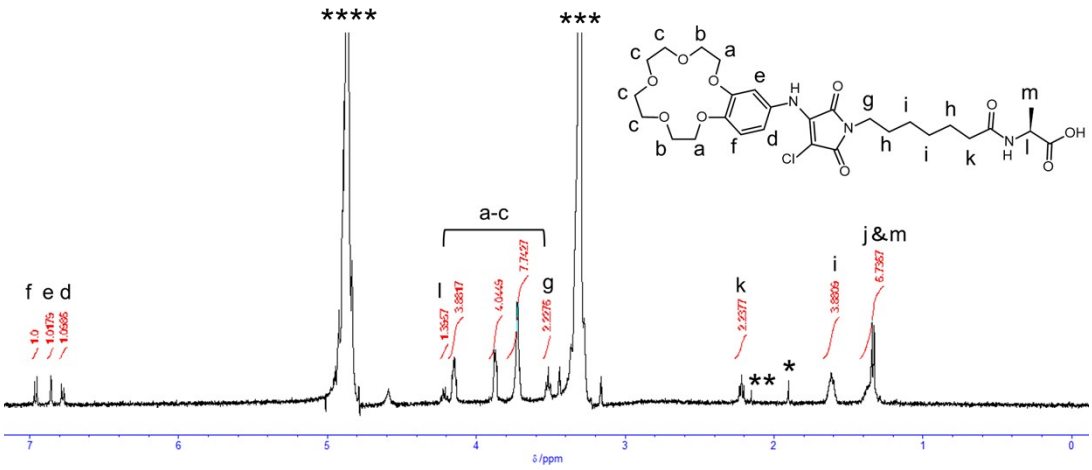

Figure S10. ^{1}H NMR spectrum (500 MHz, CD_3OD) of **B15C5-AAC-C6-L-Ala**. The peaks labelled with *, ** correspond to minor solvent impurities; *** indicates the residual non-deuterated solvent signal; and **** denotes residual water.

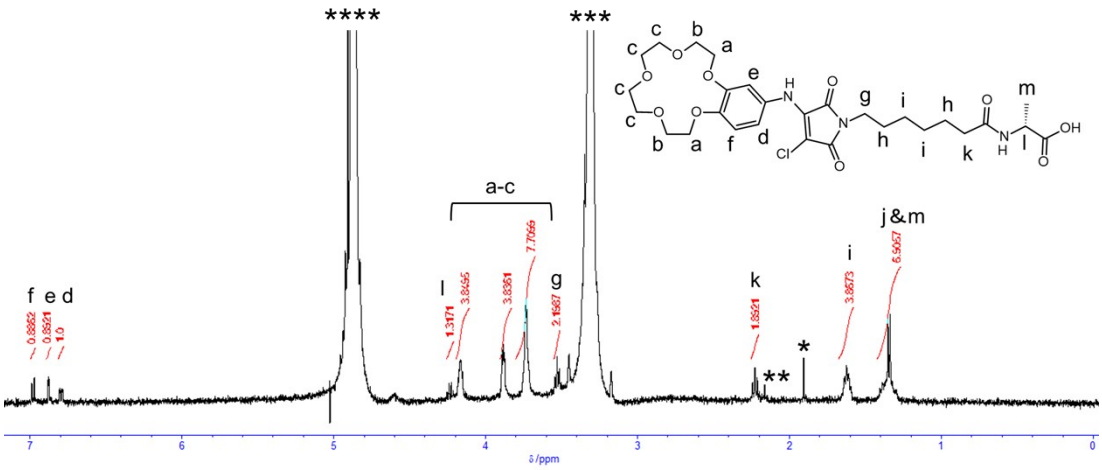

Figure S11. ^{1}H NMR spectrum (500 MHz, CD_3OD) of **B15C5-AAC-C6-D-Ala**. The peaks labelled with *, ** correspond to minor solvent impurities; *** indicates the residual non-deuterated solvent signal; and **** denotes residual water.

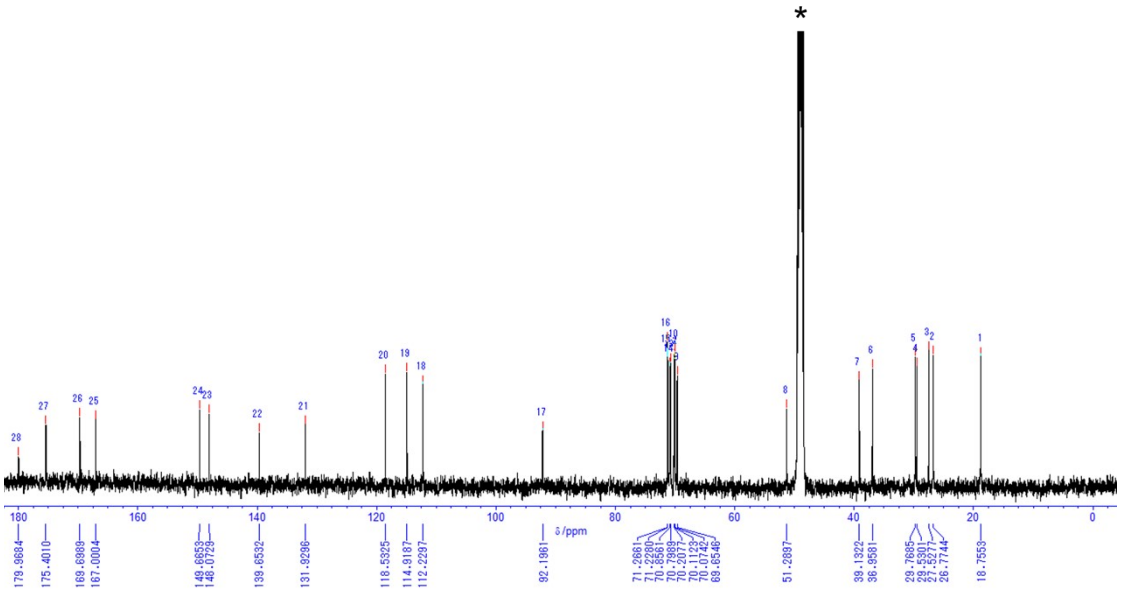

Figure S12. ^{13}C NMR spectrum (125 MHz, CD_3OD) of **B15C5-AAC-C6-L-Ala**. The peak labelled with an asterisk is attributed to residual non-deuterated solvent.

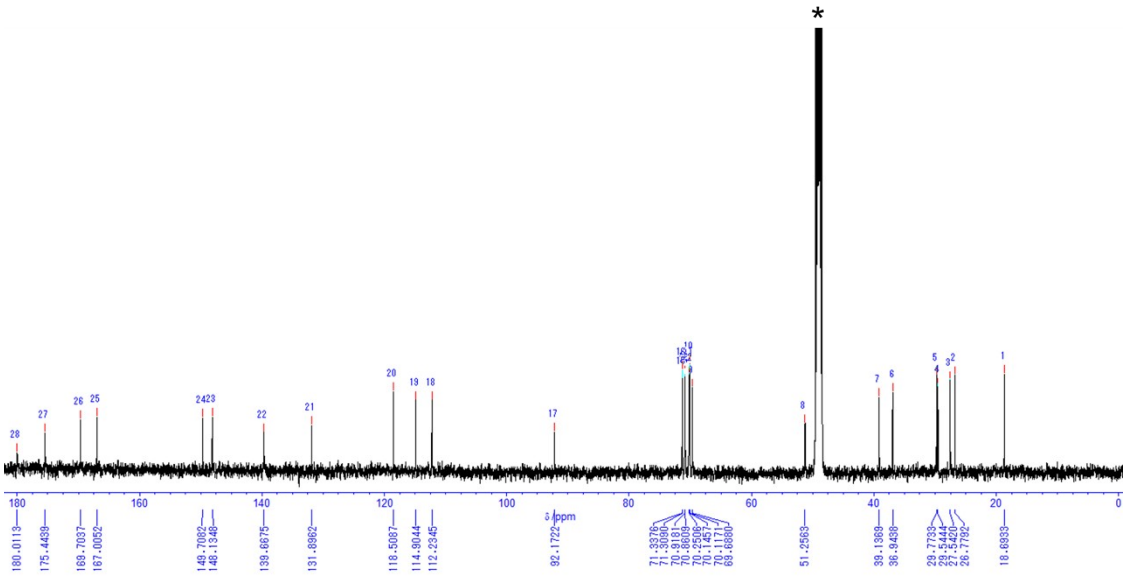

Figure S13. ^{13}C NMR spectrum (125 MHz, CD_3OD) of **B15C5-AAC-C6-D-Ala**. The peak labelled with an asterisk is attributed to residual non-deuterated solvent.

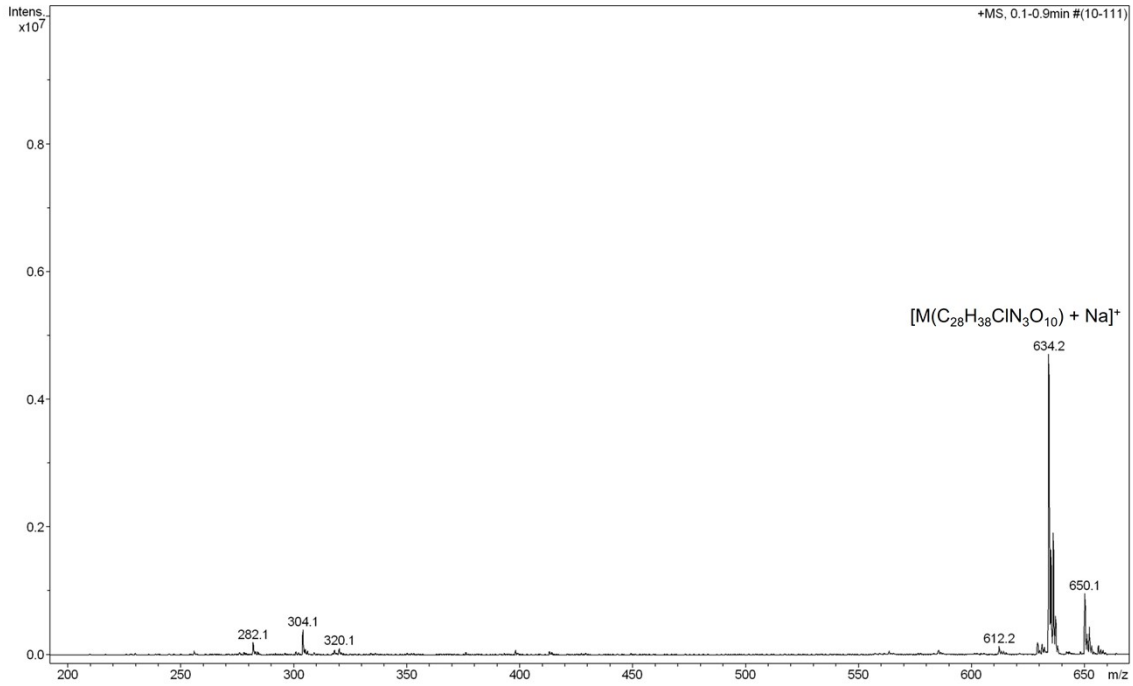

Figure S14. LRMS spectrum of **B15C5-AAC-C6-L-Ala** (ESI, positive mode).

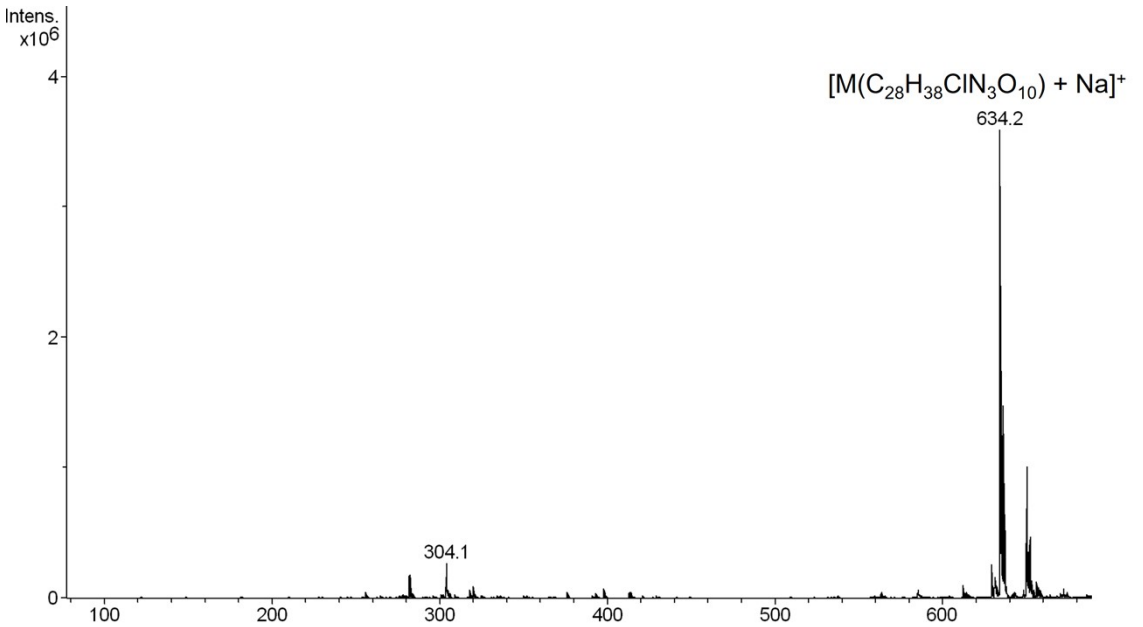

Figure S15. LRMS spectrum of **B15C5-AAC-C6-D-Ala** (ESI, positive mode).

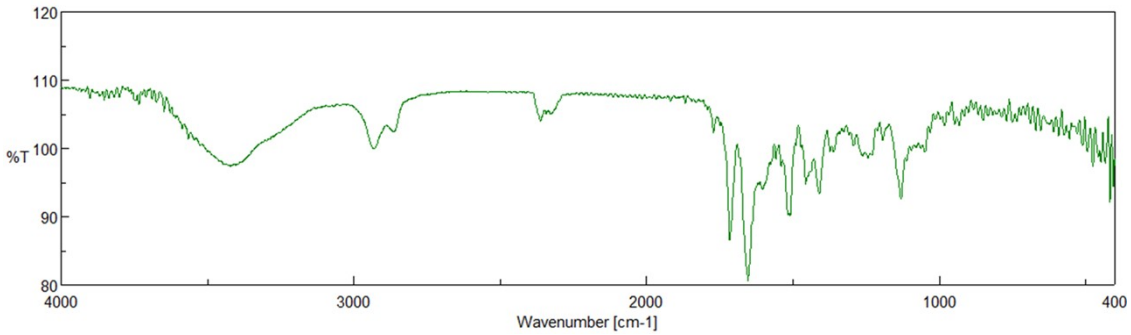

Figure S15. IR (KBr pellet) spectrum of **B15C5-AAC-C6-L-Ala** (ESI, positive mode).

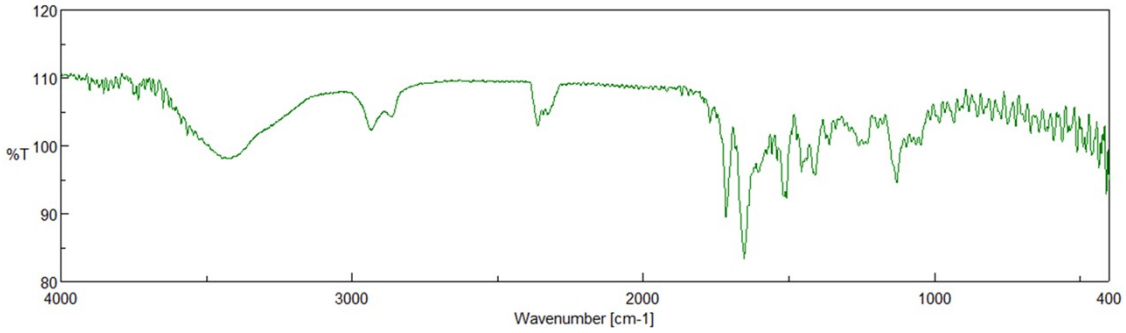

Figure S16. IR (KBr pellet) spectrum of **B15C5-AAC-C6-D-Ala** (ESI, positive mode).

References

1. M. J. Frisch, G. W. Trucks, H. B. Schlegel, G. E. Scuseria, M. A. Robb, J. R. Cheeseman, G. Scalmani, V. Barone, G. A. Petersson, H. Nakatsuji, X. Li, M. Caricato, A. V. Marenich, J. Bloino, B. G. Janesko, R. Gomperts, B. Mennucci, H. P. Hratchian, J. V. Ortiz, A. F. Izmaylov, J. L. Sonnenberg, D. Williams-Young, F. Ding, F. Lipparini, F. Egidi, J. Goings, B. Peng, A. Petrone, T. Henderson, D. Ranasinghe, V. G. Zakrzewski, J. Gao, N. Rega, G. Zheng, W. Liang, M. Hada, M. Ehara, K. Toyota, R. Fukuda, J. Hasegawa, M. Ishida, T. Nakajima, Y. Honda, O. Kitao, H. Nakai, T. Vreven, K. Throssell, J. A. Montgomery Jr., J. E. Peralta, F. Ogliaro, M. J. Bearpark, J. J. Heyd, E. N. Brothers, K. N. Kudin, V. N. Staroverov, T. A. Keith, R. Kobayashi, J. Normand, K. Raghavachari, A. P. Rendell, J. C. Burant, S. S. Iyengar, J. Tomasi, M. Cosso, J. M. Millam, M. Klene, C. Adamo, R. Cammi, J. W. Ochterski, R. L. Martin,

K. Morokuma, O. Farkas, J. B. Foresman and D. J. Fox, Gaussian 16W (Revision A.03), Gaussian, Inc.: Wallingford CT, 2016.

2. S. Grimme, J. Antony, S. Ehrlich and H. Krieg, *J. Chem. Phys.*, 2010, **132**, 154104.
3. G. A. Petersson and M. A. Al-Laham, *J. Chem. Phys.*, 1991, **94**, 6081.
4. C. C. Wilson, D. Myles, M. Ghosh, L. N. Johnson and W. Wang, *New J. Chem.*, 2005, **29**, 1318.
5. M. J. Frisch, G. W. Trucks, H. B. Schlegel, G. E. Scuseria, M. A. Robb, J. R. Cheeseman, G. Scalmani, V. Barone, G. A. Petersson, H. Nakatsuji, X. Li, M. Caricato, A. V. Marenich, J. Bloino, B. G. Janesko, R. Gomperts, B. Mennucci, H. P. Hratchian, J. V. Ortiz, A. F. Izmaylov, J. L. Sonnenberg, D. Williams-Young, F. Ding, F. Lipparini, F. Egidi, J. Goings, B. Peng, A. Petrone, T. Henderson, D. Ranasinghe, V. G. Zakrzewski, J. Gao, N. Rega, G. Zheng, W. Liang, M. Hada, M. Ehara, K. Toyota, R. Fukuda, J. Hasegawa, M. Ishida, T. Nakajima, Y. Honda, O. Kitao, H. Nakai, T. Vreven, K. Throssell, J. A. Montgomery, Jr., J. E. Peralta, F. Ogliaro, M. J. Bearpark, J. J. Heyd, E. N. Brothers, K. N. Kudin, V. N. Staroverov, T. A. Keith, R. Kobayashi, J. Normand, K. Raghavachari, A. P. Rendell, J. C. Burant, S. S. Iyengar, J. Tomasi, M. Cossi, J. M. Millam, M. Klene, C. Adamo, R. Cammi, J. W. Ochterski, R. L. Martin, K. Morokuma, O. Farkas, J. B. Foresman, and D. J. Fox, Gaussian 16W (Revision C.02), Gaussian, Inc.: Wallingford CT, 2019.
6. R. Oosumi, M. Ikeda, A. Ito, M. Izumi and R. Ochi, *Soft Matter*, 2020, **16**, 7274.
7. Y. Chabatake, T. Tanigawa, Y. Hirayama, R. Taniguchi, A. Ito, K. Takahashi, S. Noro, T. Akutagawa, T. Nakamura, M. Izumi and R. Ochi, *Soft Matter*, 2024, **20**, 8170.